Journal of Clinical and Translational Hepatology **2022** vol. 10(1) | 34–41
DOI: 10.14218/JCTH.2021.00053

Original Article

Added Value of Quantitative Apparent Diffusion Coefficients for Identifying Small Hepatocellular Carcinoma from Benign Nodule Categorized as LI-RADS 3 and 4 in Cirrhosis

Xi Zhong[1#], Hongsheng Tang[2#], Tianpei Guan[2], Bingui Lu[1], Chuangjia Zhang[1], Danlei Tang[1], Jiansheng Li[1*] and Shuzhong Cui[2*]

[1]Department of Medical Imaging, Affiliated Cancer Hospital & Institute of Guangzhou Medical University, Guangzhou, Guangdong, China; [2]Department of Abdominal Surgery, Affiliated Cancer Hospital & Institute of Guangzhou Medical University, Guangzhou, Guangdong, China

Received: 4 February 2021 | **Revised:** 19 April 2021 | **Accepted:** 26 April 2021 | **Published:** 28 May 2021

Abstract

Background and Aims: Correct identification of small hepatocellular carcinomas (HCCs) and benign nodules in cirrhosis remains challenging, quantitative apparent diffusion coefficients (ADCs) have shown potential value in characterization of benign and malignant liver lesions. We aimed to explore the added value of ADCs in the identification of small (≤3 cm) HCCs and benign nodules categorized as Liver Imaging Reporting and Data System (LI-RADS) 3 (LR-3) and 4 (LR-4) in cirrhosis. ***Methods:*** Ninety-seven cirrhosis patients with 109 small nodules (70 HCCs, 39 benign nodules) of LR-3 and 4 LR-4 based on major and ancillary magnetic resonance imaging features were included. Multiparametric quantitative ADCs of the lesions, including the mean ADC (ADC_{mean}), minimum ADC (ADC_{min}), maximal ADC (ADC_{max}), ADC standard deviation (ADC_{std}), and mean ADC value ratio of lesion-to-liver parenchyma (ADC_{ratio}) were calculated. Regarding the joint diagnosis, a nomogram model was plotted using multivariate logistic regression analysis. The performance was assessed using the area under the receiver operating characteristic curve (AUC). ***Results:*** The ADC_{mean}, ADC_{min}, ADC_{ratio}, and ADC_{std} were significantly associated with the identification of small HCC and benign nodules (p<0.001). For the joint diagnosis, the LI-RADS category (odds ratio [OR]=12.50), ADC_{min} (OR=0.14), and ADC_{ratio} (OR=0.12) were identified as independent factors for distinguishing HCCs from benign nodules. The joint nomogram model showed good calibration and discrimination, with a C-index of 0.947. Compared with the LI-RADS category alone, this nomogram model demonstrated a significant improvement in diagnostic performance, with AUC increasing from 0.820 to 0.967 (p=0.001). ***Conclusions:*** The addition of quantitative ADCs could improve the identification of small HCC and benign nodules categorized as LR-3 and 4 LR-4 in patients with cirrhosis.

Citation of this article: Zhong X, Tang H, Guan T, Lu B, Zhang C, Tang D, *et al*. Added Value of Quantitative Apparent Diffusion Coefficients for Identifying Small Hepatocellular Carcinoma from Benign Nodule Categorized as LI-RADS 3 and 4 in Cirrhosis. J Clin Transl Hepatol 2022;10(1):34–41. doi: 10.14218/JCTH.2021.00053.

Keywords: Hepatocellular carcinoma; Liver cirrhosis; Liver imaging reporting and data system; Magnetic resonance imaging; diagnosis.

Abbreviations: ADC, apparent diffusion coefficient; ADC_{mean}, mean ADC; ADC_{min}, minimum ADC; ADC_{max}, maximal ADC; ADC_{ratio}, mean ADC value ratio of lesion-to-liver parenchyma; ADC_{std}, ADC standard deviation; AUC, area under the receiver operating characteristic curve; CI, confidence interval; DWI, diffusion-weighted magnetic resonance imaging; FA, flip angle; FOV, field of view; Gd-DTPA, gadolinium diethylenetriamine pentaacetic acid; HCC, hepatocellular carcinoma; ICCs, interclass correlation coefficients; LI-RADS, liver imaging reporting and data system; MRI, magnetic resonance imaging; OR, odds ratio; ROC, receiver operating characteristic curve; ROI, region of interest; TR/TE, repetition time/echo times.

[#]Contributed equally to this work.

[*]**Correspondence to:** Shuzhong Cui, Department of Abdominal Surgery, Affiliated Cancer Hospital & Institute of Guangzhou Medical University, Guangzhou, Guangdong 510095, China. ORCID: https://orcid.org/0000-0003-2178-8741. Tel/Fax: +86-20-6667-3666, E-mail: cuishuzhong@gzhmu.edu.cn; Jiansheng Li, Department of Medical Imaging, Affiliated Cancer Hospital & Institute of Guangzhou Medical University, Guangzhou, Guangdong 510095, China. ORCID: https://orcid.org/0000-0002-8144-3430. Tel/Fax: +86-20-6667-3636, E-mail: lijiansheng@gzhmu.edu.cn

Introduction

Hepatocellular carcinoma (HCC) is the second leading cause of cancer-related mortality worldwide, and in more than 90% of the cases HCC has been reported to be associated with cirrhosis.[1] Early detection of HCC is crucial for effective treatment and patients' long-term survival.[1–3] Recently, the Liver Imaging Reporting and Data System (LI-RADS) has been widely used to standardize terminology and criteria for detecting HCC in high-risk patients.[4–9]

LI-RADS categories reflect the relative probability of HCC development, whereby categories ranging from LR-1 (definitely benign) to LR-5 (definitely HCC) and LR-TIV (definite tumor in vein) are assigned based on the presence of specific imaging features.[5,6] Ancillary features, such as restricted diffusion, mild-moderate T2 hyperintensity, and hepatobiliary phase hypointensity, have been identified as helpful findings that could be used to improve characterization and detection, promote confidence, and modify the LI-RADS category. Although, it is widely believed that ancillary features may facilitate the characterization of cirrhotic nodules,[4,7,8,10,11] their use to upgrade the category from LR-4 to LR-5 is not permitted.[6,12] Thus, correct identification of HCCs and benign nodules with LI-RADS categories 3 and 4

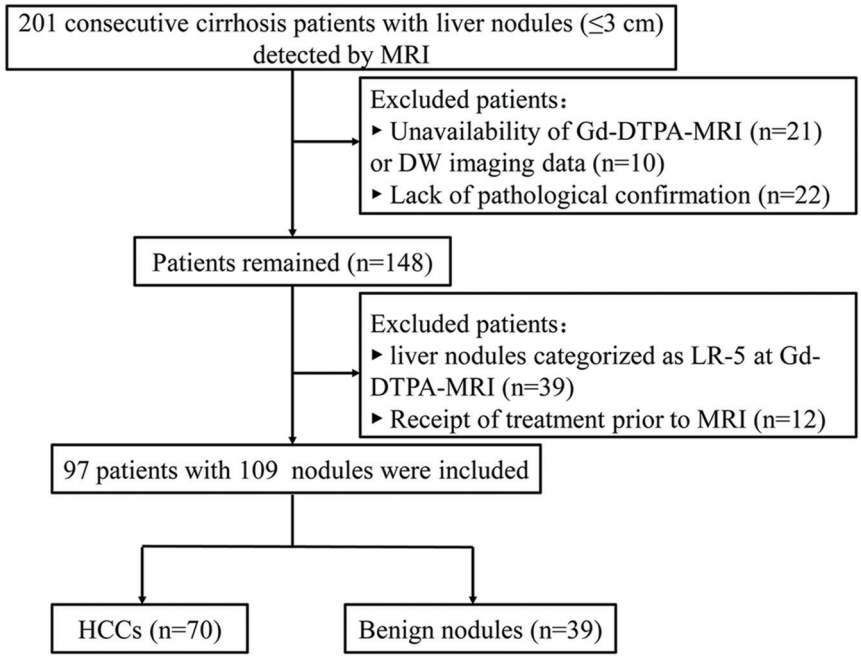

Fig. 1. Flowchart of the study population.

remains challenging.

Diffusion-weighted imaging (DWI) is a functional magnetic resonance imaging (MRI) technique that enables the characterization of biological tissues. Apparent diffusion coefficient (ADC) values quantitatively reflect the diffusion attributes of water molecules. It has shown potential value in the characterization of benign and malignant liver nodules.[13–15] Moreover, recent studies have suggested that ADC may be useful in predicting histopathological differentiation,[16] microvascular invasion,[17] and early recurrence of HCC.[18] Among the quantitative ADC values, mean ADC (ADC_{mean}) is commonly selected.[19] Several studies have suggested that the ADC ratio (ADC_{ratio}; mean ADC of the lesion-to-liver parenchyma) or minimum ADC (ADC_{min}) may also show potential for identifying HCCs or predicting the histological grade of HCCs.[14,15,20] To our knowledge, whether ADCs have additive value to LI-RADS criteria in the discrimination of benign and malignant liver lesions is unclear. Thus, in this study, we sought to determine the additive value of quantitative ADCs for the identification of small HCC and benign nodules categorized as LR-3 and LR-4 in a cirrhotic liver.

Methods

Patient population

This retrospective study was approved by the institutional review board of the Affiliated Cancer Hospital & Institute of Guangzhou Medical University. Between January 2015 and December 2019, a total of 201 consecutive cirrhosis patients with liver nodules smaller than or equivalent to 3 cm detected on MRI were identified. The patients' MRI, clinical and histopathology data were reviewed. The inclusion criteria were as follows: (1) patients who had undergone dynamic gadolinium diethylenetriamine pentaacetic acid (Gd-DTPA) enhancement and DWI; (2) patients in whom pathological confirmation had been performed after surgery or biopsy; (3) patients with liver nodules categorized as LR-3 or LR-4 based on the combination of major and ancillary features; and (4) patients who did not undergo any treatment before MRI. One hundred and two patients were excluded due to the following reasons: (1) unavailability of Gd-DTPA-MRI (*n*=21, underwent gadoxetic acid-enhanced MRI) or DWI data (*n*=10); (2) lack of pathological confirmation (*n*=22); (3) presence of liver nodules categorized as LR-5 (definitely HCC) (*n*=39); and (4) receipt of treatment prior to MRI (*n*=12). Finally, 97 patients (74 men, 23 women; aged 34 to 80 years) with 109 small nodules (*n*=70, HCCs; *n*=39, benign nodules) were included. The patient inclusion flowchart is shown in Figure 1.

MRI techniques

All MR images were obtained using a 3.0-T whole-body MR system (Achieva; Philips Healthcare, Amsterdam, Netherland) with a 16-channel phased-array coil. Scanning sequences included a dual gradient-recalled echo T1-weighted sequence (repetition time/echo times [TR/TE], 180/2.4–5.2 ms; flip angle [FA], 70°; field of view (FOV), 35×32 cm; matrix, 384×225; and slice thickness, 5 mm); axial T2-weighted fat-suppression turbo spin-echo sequence (TR/TE, 3,500–4,800/75 ms; FA, 120°; matrix, 384×225; FOV, 350×320 cm; slice thickness, 5 mm); and dynamic contrast-enhanced MRI performed using a T1-weighted 3D turbo-field-echo sequence (T1 high-resolution isotropic volume examination; THRIVE, Philips Healthcare) (TR/TE=3.9/1.85 ms, 35×32 cm; matrix, 384×225; FA, 10°; slice thickness, 5 mm; spacing=2 mm). After scanning unenhanced T1-weighted images, 0.1 mmol/kg Gd-DTPA (Magnevist; Schering, Berlin, Germany) was administered intravenously via an antecubital venous catheter at a rate of 2.0 mL/s, followed by a 20-mL saline flush at a similar rate by using a power injector. Thereafter, arterial-phase (20~35 s), portal-phase (60 s), and delayed-phase (3-m) images were obtained. DWI was performed before contrast-enhanced MRI by using a respiratory-triggered single-shot echo-planar sequence with b-values of 0 and 800 s/

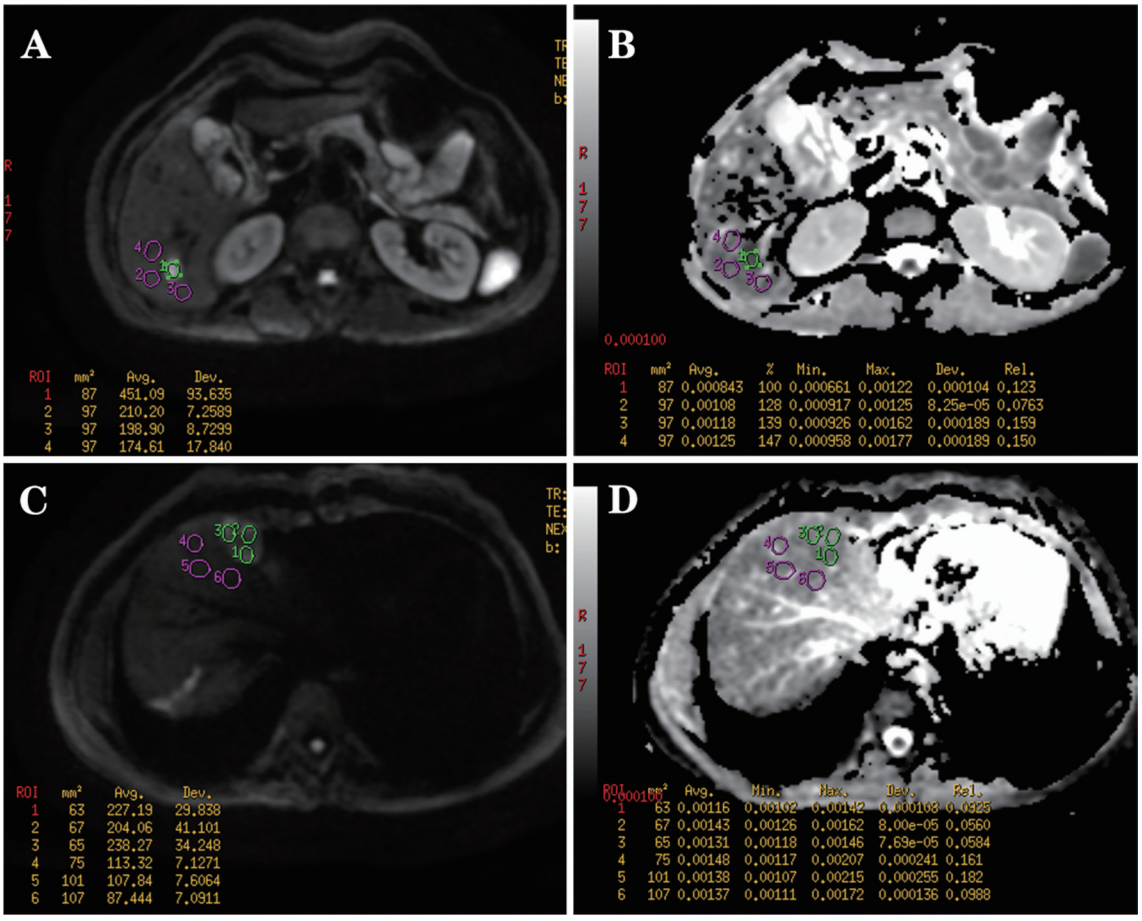

Fig. 2. Schematic diagram of the ADC measurement. (A–B) ADC parameter measurement for lesions with diameter ≤2 cm; only one circular ROI was placed (green circle), and as much of the volume of the lesion as possible was encompassed in the ROI. (C–D) For nodules with diameter >2 cm, three ROIs with an equivalent area were randomly placed inside the lesion (green circle), and the ADC parameters generated in ROIs were averaged for analysis. For ADC measurement of liver parenchyma, three circular ROIs ≈ 1 cm^2 were randomly placed in the surrounding liver parenchyma (purple circle), vessels and bile ducts were carefully avoided, the mean ADC generated in the ROIs was averaged, and ADC_{ratio} [lesion to liver] was calculated for analysis. ADC, apparent diffusion coefficient; ADC_{ratio}, mean ADC value ratio of lesion-to-liver parenchyma; ROI, region of interest.

mm^2 (TR/TE, 1,000/65; FA, 90°; FOV, 35×32 cm; matrix, 128×128; section thickness, 5 mm, and intersection gap 1 mm). Quantitative ADC maps were derived automatically by using commercially available software and an imaging workstation. ADC maps were generated automatically on a voxel-by-voxel basis from the two b-values.

Qualitative image analysis

Two radiologists independently analyzed all images and reached a consensus. Observer 1 (CJZ, with 3 years of MRI diagnosis experience) and observer 2 (BGL, with 10 years of MRI diagnosis experience) were informed that this study attempted to evaluate the contribution of LI-RADS categories of HCCs based on major and ancillary features; however, they were blinded to the patients' clinical data and pathologic diagnosis. The criteria for MRI features and LI-RADS categories were based on LI-RADS v2018.[6]

Quantitative analysis

Quantitative ADC values were independently measured on ADC maps by two radiologists (XZ with 6 years of image processing experience; DLT with 3 years of image processing experience). The mean ADC (ADC_{mean}, minimum ADC (ADC_{min}), maximal ADC (ADC_{max}), and ADC standard deviation (ADC_{std}) of the nodules were documented. Furthermore, ADCs of the surrounding liver parenchyma were also assessed, and the mean ADC value ratio of lesion-to-liver parenchyma (ADC_{ratio} [lesion to liver]) was calculated.[14,15] The interobserver reproducibility of ADC measurement was evaluated using interclass correlation coefficients (ICCs). An ICC value of ≥0.75 indicated good agreement for measurement, and ADC values from the two measurements were averaged for analysis. If the ICC value was <0.75, ADC values from the two measurements were independently used for analysis.

Regarding ADC measurement for lesions, we classified the ADC assessment into two groups.[15] (1) Only one circular region of interest (ROI) was determined for lesions with a diameter of ≤2 cm, and as much of the volume of the lesion as possible was encompassed in the ROI **(**Fig. 2A–B**)** before the ROI was copied to the surrounding liver parenchyma. (2) For nodules with a diameter of >2 cm, three ROIs with an equivalent area were randomly placed inside the lesion, and the ADC parameters generated in the ROIs were averaged for analysis (Fig. 2 C–D). In both groups, areas of

intratumoral hemorrhage or necrosis were avoided. When a nodule was difficult to identify on ADC maps, contrast-enhanced T1-weighted images were used for accurate ROI placement. To minimize the influence of a partial volume averaging effect and motion artefacts, the slice depicting the maximum diameter of the nodule was selected for ADC measurement.

For ADC measurement of liver parenchyma, three circular ROIs ≈1 cm^2 were randomly placed in surrounding liver parenchyma; vessels and bile ducts were carefully avoided. The mean ADC generated for the ROIs was averaged, and the ADC ratio (mean ADC of lesion to the liver) was calculated.

Nomogram model development

The diagnostic efficacy of LI-RADS and ADC parameters was evaluated by using univariate analysis. The variables showing statistical differences were reserved for further analysis, and binary logistic regression analysis was performed to determine the independent parameters in the differentiation of HCC and benign nodules. These variables were screened using the backward stepwise selection method, and the likelihood ratio test with Akaike's information criterion was identified as the stopping rule.[21] A nomogram model was developed on the basis of the independent variables, and the diagnostic performance of the nomogram was assessed by a receiver operating characteristic (ROC) curve. A calibration curve was also plotted to assess the degree of fitting of the nomogram by using the Hosmer-Lemeshow test.[22]

Statistical analysis

The construction and calibration plots of the nomogram model were obtained using the "rms" package of R statistical software (version 3.3.1 http://www.rproject.org/). The other statistical tests were performed using the SPSS 16.0 software package (SPSS Inc., Chicago, IL, USA). Statistical significance was accepted for p <0.05.

Inter-reader variability between the two observers for LI-RADS categories was assessed using kappa statistics. Classification of validity based on the k-values was performed as follows:[9] very good (1≥k>0.8); good (0.8≥k>0.6); moderate (0.6≥k>0.4); fair (0.4≥k>0.2); or poor (0.2≥k>0). Categorical variables were expressed as numbers, and quantitative ADC parameters and ADC ratio were expressed as mean and standard deviation. Univariate analysis for the ADC parameters was performed by ROC analysis, and multivariate analysis was performed by multivariate logistic regression analysis. The overall diagnostic efficiency of each approach was evaluated on the basis of the area under the ROC (AUC), and AUC comparisons were performed using the McNemar test, while comparisons of sensitivity and specificity were performed using the Pearson chi-square test (or Fisher test).

Results

Clinical characteristics of the patients

The detailed characteristics of the patients and lesions are displayed in Table 1. A total of 97 patients (74 males, 23 females; age 34 to 80 years) with cirrhosis confirmed by histopathology were included. The etiological factor responsible for the cirrhosis was hepatitis B virus infection in 78 cases, hepatitis C virus infection in 13 cases, and alcohol abuse in six cases. The alpha-fetoprotein level was <200 ng/mL in 76 cases, ≥200 ng/mL in 12 cases, and unobtainable in 9 cases.

Table 1. Characteristics of patients and lesions

Characteristic	HCCs	Benign nodules
Patient characteristic		
Number	65	32
Age in years	56.1±9.8	57.8±9.6
Gender		
Male	47	27
Female	18	5
Child-Pugh class		
A	48	23
B	14	8
C	3	1
AFP serum		
< 200 ng/mL	52	24
≥200 ng/mL	10	2
Unobtainable	3	6
Etiology of liver cirrhosis		
HBV infection	51	27
HCV infection	9	4
Alcohol consumption	5	1
Lesion characteristic		
Number	70	39
Nodule size in cm	2.0±0.6	1.8±0.5
Histopathology features		
Well-differentiated HCC	34	0
Moderately differentiated HCC	29	0
Poorly differentiated HCC	7	0
Dysplastic nodule	0	34
Regenerative nodule	0	4
Hepatic adenoma	0	1
Diagnosis method		
Surgery	59	18
Percutaneous biopsy	11	21

AFP, alpha fetoprotein; HBV, hepatitis B virus; HCC, hepatocellular carcinoma; HCV, hepatitis C virus.

A total of 109 small nodules with LR-3 and LR-4 were included. According to the pathologic analysis, 70 nodules were diagnosed as HCCs and 39 lesions were benign nodules. Sixty-three patients showed only HCCs, with the following distribution of lesions: patients with one lesion (n=59), two lesions (n=3), and three lesions (n=1). In contrast, 32 patients showed only benign nodules with the following distribution: patients with one lesion (n=28) and those with two lesions (n=4). Two patients were diagnosed with both HCCs and benign nodules, including one patient with two lesions (HCC, n=1; benign nodule, n=1) and one

Table 2. Comparison of quantitative ADC parameters between HCCs and benign nodules

Parameter	HCCs, *n*=70	Benign nodules, *n*=39	*p*	ICC
ADC_{mean} ($\times10^{-6}$ mm^2/s)	1,071.6±131.7	1,179.8±1,501.7	<0.001	0.83
ADC_{min} ($\times10^{-6}$ mm^2/s)	823.9±101.4	982.7±125.1	<0.001	0.77
ADC_{max} ($\times10^{-6}$ mm^2/s)	1,393.6±170.2	1,421.3±187.5	0.467	0.81
ADC_{std} ($\times10^{-6}$ mm^2/s)	166.5±104.1	93.9±66.0	<0.001	0.78
ADC_{ratio} (lesion to liver)	0.87±0.13	1.39±0.19	<0.001	0.88

ADC, apparent diffusion coefficient; ADC_{mean}, mean ADC; ADC_{min}, minimum ADC; ADC_{max}, maximal ADC; ADC_{ratio}, mean ADC value ratio of lesion-to-liver parenchyma; ADC_{std}, ADC standard deviation; HCC, hepatocellular carcinoma.

patient with three lesions (HCC, *n*=1; benign nodules, *n*=2). A total of 70 HCCs (diameter range, 1.3–3.0 cm; mean, 2.0 cm) and 39 benign nodules (diameter range, 1.1–2.7 cm; mean, 1.8 cm) were identified.

Diagnostic performance of LI-RADS criteria

Inter-observer agreement for LI-RADS categories between the two observers was determined to be very good (k=0.89). Based on the results in consensus, of the 70 HCCs, 59 lesions were categorized as LR-4, and 11 lesions were categorized as LR-3. Of the 39 benign nodules, 30 lesions were categorized as LR-3, and 9 lesions were categorized as LR-4. For the differentiation of HCC and benign nodules by using ROC analysis, LR-4 demonstrated an AUC value of 0.820 (95% confidence interval [CI]: 0.730, 0.910), sensitivity of 84.3% (59/70), and specificity of 76.9% (30/39).

Diagnostic performance of quantitative ADC values

As shown in Table 2, the interobserver reproducibility of each ADC parameter measurement showed good agreement, with ICC values ranging from 0.77 to 0.88; the ADC values from the two measurements were averaged for analysis. The ADC_{mean}, ADC_{min}, and ADC_{ratio} (lesion to liver) of HCCs were all significantly lower than those of benign nodules (p<0.001); ROC analysis showed that the AUC values ranged from 0.756 to 0.891 for the differentiation of HCC and benign nodules (Fig. 3A). The ADC_{std} of HCCs was significantly higher than that of benign nodules (p<0.001), and ROC analysis showed that the AUC value was 0.854 (Fig. 3B). No significant difference was noted in ADC_{max} between HCCs and benign nodules (p=0.467). The diagnostic performance of ADC parameters with statistically significant differences is summarized in Table 3; the ADC_{min} showed optimal diagnostic efficacy with a cut-off value of 858×10^{-6} mm^2/s, sensitivity of 91.4% (64/70), and specificity of 84.6% (33/39).

Additive diagnostic value of quantitative ADC values

The LI-RADS category and quantitative variables (ADC_{mean}, ADC_{min}, ADC_{std}) and ADC_{ratio} (lesion to liver) were selected to identify the independent factors associated with differentiation of HCC and benign nodules. Multivariate analysis showed that the LI-RADS category (odds ratio [OR]=12.50, 95% CI: 3.86~23.30), ADC_{min} (OR=0.14, 95% CI: 0.05~0.38), and ADC_{ratio} (lesion to liver) (OR=0.12, 95% CI: 0.03~0.39) were the independent factors (Table 4). Based on the three independent factors, a nomogram model was constructed (Fig. 4A), and the calibration curve of the nomogram (Fig.

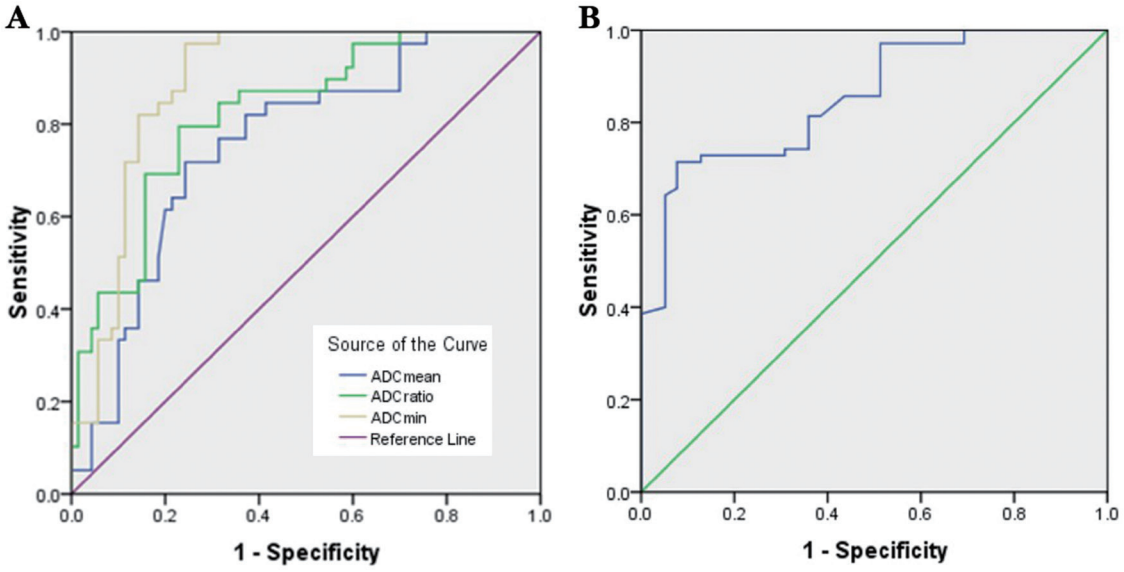

Fig. 3. ROC analysis of ADC parameters in distinguishing small HCCs from benign nodules with LR-3 and LR-4. (A) ROC analysis for ADC_{mean}, ADC_{ratio} and ADC_{min}. (B) ROC analysis for ADC_{std}. ADC, apparent diffusion coefficient; ADC_{mean}, mean ADC; ADC_{min}, minimum ADC; ADC_{ratio}, mean ADC value ratio of lesion-to-liver parenchyma; ADC_{std}, ADC standard deviation; HCC, hepatocellular carcinoma; ROC, receiver operating characteristic curve.

Table 3. Performance evaluation of quantitative ADC parameters for differentiating HCCs and benign nodules

Parameter	Cut-off value	AUC (95% CI)	Sensitivity	Specificity
ADC_{mean} ($\times10^{-6}$ mm^2/s)	1,072	0.756 (0.663–0.849)	78.6% (55/70)	69.2% (27/39)
ADC_{min} ($\times10^{-6}$ mm^2/s)	858	0.891 (0.830–0.952)	91.4% (64/70)	84.6% (33/39)
ADC_{std} ($\times10^{-6}$ mm^2/s)	98	0.854 (0.784–0.924)	88.6% (62/70)	79.5% (31/39)
ADC_{ratio} (lesion to liver)	0.91	0.824 (0.745–0.903)	84.3% (59/70)	79.5% (31/39)

ADC, apparent diffusion coefficient; ADC_{mean}, mean ADC; ADC_{min}, minimum ADC; ADC_{ratio}, mean ADC value ratio of lesion-to-liver parenchyma; ADC_{std}, ADC standard deviation; HCC, hepatocellular carcinoma.

Table 4. Results of multivariate analysis for nomogram model construction

Parameter	Coefficient	OR (95% CI)	*p*
Intercept	21.309	–	<0.001
LI-RADS category	2.886	12.50 (3.86–23.30)	<0.001
ADC_{min}	−0.013	0.14 (0.05–0.38)	0.005
ADC_{ratio} (lesion to liver)	−11.189	0.12 (0.03–0.39)	<0.001

ADC_{min}, minimum ADC; ADC_{ratio}, mean ADC value ratio of lesion-to-liver parenchyma; LI-RADS, liver imaging reporting and data system.

4B) was plotted. The joint nomogram model showed good calibration and discrimination, with a C-index of 0.947. As shown in Table 4, a formula obtained from the three parameters weighted by their coefficients was constructed: diagnosis score=21.309+(2.886×LI-RADS category)−(0.013 ×ADC_{min})−(11.189×ADC_{ratio} [lesion to liver]). Based on the diagnosis scores, the performance of the nomogram model was determined by using ROC analysis.

In comparison with the LI-RADS category alone, the combined nomogram model demonstrated a significant

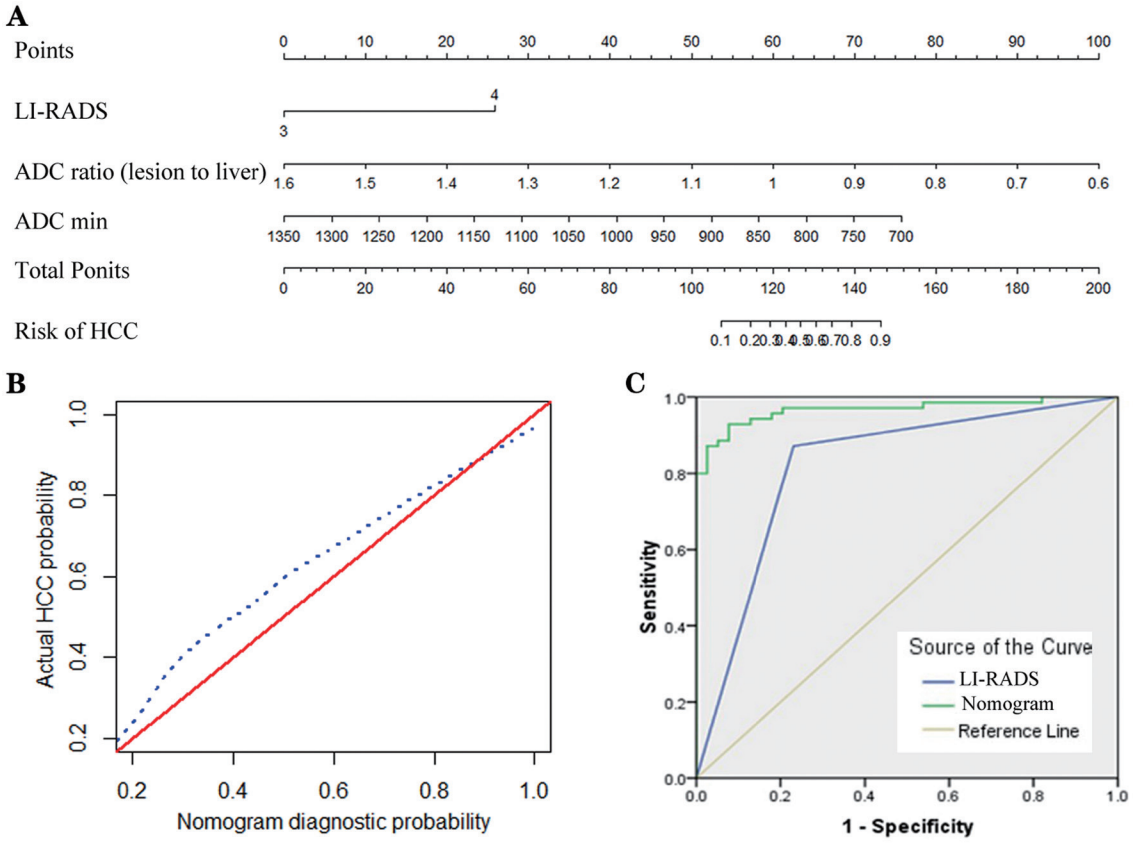

Fig. 4. Nomogram construction, calibration, and performance assessment. (A) The LI-RADS, ADC_{ratio} [lesion to liver], and ADC_{min} were combined to plot the nomogram. (B) Calibration curves of the radiomics nomogram; the 45° red full line represents a perfect diagnosis, and the dotted blue lines represent the actual diagnosis performance of the nomogram. (C) ROC analysis showed that the combined nomogram model demonstrated good classification performance. ADC_{ratio}, mean ADC value ratio of lesion-to-liver parenchyma; ADC_{min}, minimum ADC; LI-RADS, liver imaging reporting and data system; ROC, receiver operating characteristic curve.

improvement in diagnostic performance for differentiating HCCs and benign nodules with LR-3 and LR-4 (Fig. 4C), with the AUC increasing from 0.820 (95% CI: 0.730–0.910) to 0.967 (95% CI: 0.936–0.998) (p=0.001), sensitivity increasing 84.3% from to 95.7% (p=0.045), and specificity increasing from 76.9% to 97.4% (p=0.014).

Discussion

In the present study, we explored the additive value of quantitative ADC values in the differentiation of small HCCs and benign nodules with LR-3 and LR-4 in Gd-DTPA-MRI of the cirrhotic liver. Several ADC parameters showed potential discriminative power, and the ADC_{min} showed the best diagnostic efficacy (AUC=0.891). The LI-RADS category, ADC_{min}, and ADC_{ratio} (lesion to the liver) were identified as independent factors for diagnosing HCCs. In comparison with the LI-RADS category alone, the combined diagnostic model showed significantly better performance, with the AUC value increasing from 0.820 to 0.967. Our findings showed that the addition of quantitative ADCs could improve the discrimination of HCCs and benign nodules categorized as LR-3 and LR-4.

The LR-5 category has been verified to show extremely high specificity (up to 96%) in the diagnosis of HCC; however, its sensitivity was only approximately 50%.[2,7] In this study, only cirrhotic nodules with LR-3 and LR-4 categories were selected for analysis, and when using LR-4 as a criterion for diagnosing HCCs, the diagnostic specificity (76.9%) was limited. We found that the ADC_{mean}, ADC_{min}, ADC_{ratio} (lesion to the liver), and ADC_{std} were significantly associated with the discrimination of small HCCs and benign nodules of LR-3 and LR-4 categories. The ADC_{min} yielded the best diagnostic performance, with an AUC of 0.891, sensitivity of 91.4%, and specificity of 84.6%. This was consistent with Lee *et al*.'s study,[18] in which the performance of ADC_{min} was significantly better than that of ADC_{mean} for identifying early recurrence of HCC.

We also found that ADC_{std} was helpful for differentiating HCC from benign nodules, and the AUC value of ADC_{std} was slightly higher than those of ADC_{mean} or ADC_{ratio} (lesion to the liver). ADC_{std} reflects the discrete distribution of signal intensity on ADC maps; thus, the significantly higher ADC_{std} of HCCs suggested that HCCs may show greater heterogeneity than benign nodules. This supported our previous studies in which MRI-based texture analysis showed potential value for the differentiation of small HCCs from dysplastic nodules.[23,24]

As a novel, noninvasive, and visual diagnosis tool, nomograms have been applied in various aspects of clinical research, including discrimination of benign and malignant diseases,[25] prediction of therapeutic response,[26] and assessment of survival prognosis.[27,28] In this study, by combining the independent contributing factors associated with the discrimination of HCCs and benign nodules, a nomogram model consisting of three factors (LI-RADS category, ADC_{min}, and ADC_{ratio} [lesion to liver]) was constructed for assessing the combined diagnosis performance of these factors. This nomogram model showed good calibration and discrimination in comparison with the LI-RADS category alone, and the nomogram demonstrated a significant improvement in diagnostic performance, with the AUC increasing from 0.820 to 0.967, sensitivity increasing from 84.3% to 95.7%, and specificity increasing from 76.9% to 97.4%. Thus, our findings provided preliminary evidence that quantitative ADCs may show additive value for identifying small HCCs and cirrhotic nodules categorized as LR-3 and LR-4 in MRI.

There are several limitations of this study. First, this was a preliminary study performed in a single center; further multicenter studies with larger sample sizes are needed to validate its clinical application. Second, although all lesions were pathologically proven, not all of them were confirmed by surgery; thus, potential selection bias cannot be ruled out. Third, although hypointensity on the hepatobiliary phase in gadoxetic acid-enhanced MRI shows good performance in identifying small HCCs,[15,24] dynamic enhancement MRI with extracellular contrast agents was selected in this study because only a few patients underwent gadoxetic acid-enhanced MRI. Finally, the cohort in this study mostly consisted of patients with HBV-associated cirrhosis and non-cirrhotic HCC was not negligible; thus, the possibility of selection bias is unavoidable.

Conclusions

Several quantitative ADC parameters helped distinguish small HCC from benign nodules in patients with cirrhosis. The addition of quantitative ADCs could improve the identification of small HCC and benign nodules categorized as LR-3 and LR-4.

Funding

This work was supported by the Guangzhou Health and Family Planning Science and Technology Project (20192A010020).

Conflict of interest

The authors have no conflict of interests related to this publication.

Author contributions

Conceived and designed the study (XZ, JL, SC), conducted the study and collected important background data (HT, TG, CZ, DT), qualitatively analyzed the medical images (BL, CZ), quantificationally analyzed the medical images (XZ, DT), drafted the manuscript (ZX, HT). All authors read and approved the final manuscript.

Data Sharing statement

The datasets used and/or analyzed during the current study are available from the corresponding author on reasonable request.

References

[1] Bertuccio P, Turati F, Carioli G, Rodriguez T, La Vecchia C, Malvezzi M, *et al*. Global trends and predictions in hepatocellular carcinoma mortality. J Hepatol 2017;67:302–309. doi:10.1259/bjr.20200743.
[2] Ronot M, Fouque O, Esvan M, Lebigot J, Aube C, Vilgrain V. Comparison of the accuracy of AASLD and LI-RADS criteria for the non-invasive diagnosis of HCC smaller than 3cm. J Hepatol 2018;68:715–723. doi:10.1016/j.jhep.2017.12.014.
[3] Torre LA, Bray F, Siegel RL, Ferlay J, Lortet-Tieulent J, Jemal A. Global cancer statistics, 2012. CA Cancer J Clin 2015;65:87–108. doi:10.3322/caac.21262.
[4] Song JS, Choi EJ, Hwang SB, Hwang HP, Choi H. LI-RADS v 2014 categorization of hepatocellular carcinoma: intraindividual comparison between gadopentetate dimeglumine-enhanced MRI and gadoxetic acid-enhanced MRI. Eur Radiol 2019;29:401–410. doi:10.1007/s00330-018-5559-z.
[5] Chernyak V, Fowler KJ, Kamaya A, Elsayes KM, Bashir MR, Kono Y, *et al*. Liver imaging reporting and data system (LI-RADS) version 2018: imaging

of hepatocellular carcinoma in at-risk patients. Radiology 2018;289:816–830. doi:10.1148/radiol.2018181494.
[6] Cerny M, Chernyak V, Olivie D, Billiard JS, Murphy-Lavallée J, Kielar AZ, *et al*. LI-RADS version 2018 ancillary features at MRI. Radiographics 2018;38:1973–2001. doi:10.1148/rg.2018180052.
[7] Cerny M, Bergeron C, Billiard JS, Murphy-Lavallée J, Olivié D, Bérubé J, *et al*. LI-RADS for MR imaging diagnosis of hepatocellular carcinoma: performance of major and ancillary features. Radiology 2018;288:118–128. doi:10.1148/radiol.201817167.
[8] Choi SH, Byun JH, Kim SY, Lee SJ, Won HJ, Shin YM, *et al*. Liver imaging reporting and data system v2014 with gadoxetate disodium-enhanced magnetic resonance imaging: validation of LI-RADS category 4 and 5 criteria. Invest Radiol 2016;51:483–490. doi:10.1097/RLI.0000000000000258.
[9] Ling W, Wang M, Ma X, Qiu T, Li J, Lu Q, *et al*. The preliminary application of liver imaging reporting and data system (LI-RADS) with contrast-enhanced ultrasound (CEUS) on small hepatic nodules (</= 2cm). J Cancer 2018;9(16):2946–2952. doi:10.7150/jca.25539.
[10] Joo I, Lee JM, Lee DH, Ahn SJ, Lee ES, Han JK. Liver imaging reporting and data system v2014 categorization of hepatocellular carcinoma on gadoxetic acid-enhanced MRI: comparison with multiphasic multidetector computed tomography. J Magn Reson Imaging 2017;45:731–740. doi:10.1002/jmri.25406.
[11] Joo I, Lee JM, Lee DH, Jeon JH, Han JK. Retrospective validation of a new diagnostic criterion for hepatocellular carcinoma on gadoxetic acid-enhanced MRI: can hypointensity on the hepatobiliary phase be used as an alternative to washout with the aid of ancillary features? Eur Radiol 2019;29:1724–1732. doi:10.1007/s00330-018-5727-1.
[12] Kielar AZ, Chernyak V, Bashir MR, Do RK, Fowler KJ, Mitchell DG, *et al*. LI-RADS 2017: an update. J Magn Reson Imaging 2018;47:1459–1474. doi:10.1002/jmri.26027.
[13] Sandrasegaran K, Tahir B, Patel A, Ramaswamy R, Bertrand K, Akisik FM, *et al*. The usefulness of diffusion-weighted imaging in the characterization of liver lesions in patients with cirrhosis. Clin Radiol 2013;68:708–715. doi:10.1016/j.crad.2012.10.023.
[14] Caraiani CN, Marian D, Militaru C, Calin A, Badea R. The role of the diffusion sequence in magnetic resonance imaging for the differential diagnosis between hepatocellular carcinoma and benign liver lesions. Clujul Med 2016;89:241–249. doi:10.15386/cjmed-567.
[15] Inchingolo R, De Gaetano AM, Curione D, Ciresa M, Miele L, Pompili M, *et al*. Role of diffusion-weighted imaging, apparent diffusion coefficient and correlation with hepatobiliary phase findings in the differentiation of hepatocellular carcinoma from dysplastic nodules in cirrhotic liver. Eur Radiol 2015;25:1087–1096. doi:10.1007/s00330-014-3500-7.
[16] Ogihara Y, Kitazume Y, Iwasa Y, Taura S, Himeno Y, Kimura T, *et al*. Prediction of histological grade of hepatocellular carcinoma using quantitative diffusion-weighted MRI: a retrospective multivendor study. Br J Radiol 2018;91:20170728. doi:10.1259/bjr.20170728.
[17] Okamura S, Sumie S, Tonan T, Nakano M, Satani M, Shimose S, *et al*. Diffusion-weighted magnetic resonance imaging predicts malignant potential in small hepatocellular carcinoma. Dig Liver Dis 2016;48:945–952. doi:10.1016/j.dld.2016.05.020.
[18] Lee S, Kim SH, Hwang JA, Lee JE, Ha SY. Pre-operative ADC predicts early recurrence of HCC after curative resection. Eur Radiol 2019;29(2):1003–1012. doi:10.1007/s00330-018-5642-5.
[19] Padhani AR, Liu G, Koh DM, Chenevert TL, Thoeny HC, Takahara T, *et al*. Diffusion-weighted magnetic resonance imaging as a cancer biomarker: consensus and recommendations. Neoplasia 2009;11:102–125. doi:10.1593/neo.81328.
[20] Nishie A, Tajima T, Asayama Y, Ishigami K, Kakihara D, Nakayama T, *et al*. Diagnostic performance of apparent diffusion coefficient for predicting histological grade of hepatocellular carcinoma. Eur J radiol 2011;80:e29–33. doi:10.1016/j.ejrad.2010.06.019.
[21] Sauerbrei W, Boulesteix AL, Binder H. Stability investigations of multivariable regression models derived from low- and high-dimensional data. J Biopharm Stat 2011;21:1206–1231. doi:10.1080/10543406.2011.629890.
[22] Kramer AA, Zimmerman JE. Assessing the calibration of mortality benchmarks in critical care: the Hosmer-Lemeshow test revisited. Crit Care Med 2007;35:2052–2056. doi:10.1097/01.CCM.0000275267.64078.B0.
[23] Zhong X, Li J, Chen Z, Yin J, Gui S, Sui Z, *et al*. Texture analysis of diffusion-weighted magnetic resonance imaging to identify atypically enhanced small hepatocellular carcinoma and dysplastic nodules under the background of cirrhosis. Chin J Hepatol 2020;28:37–42. doi:10.3760/cma.j.issn.1007-3418.2020.01.010.
[24] Zhong X, Tang H, Lu B, You J, Piao J, Yang P, *et al*. Differentiation of small hepatocellular carcinoma from dysplastic nodules in cirrhotic liver: texture analysis based on MRI improved performance in comparison over gadoxetic acid-enhanced MR and diffusion-weighted imaging. Front Oncol 2019;9:1382. doi:10.3389/fonc.2019.01382.
[25] Nie P, Yang G, Wang Z, Yan L, Miao W, Hao D, *et al*. A CT-based radiomics nomogram for differentiation of renal angiomyolipoma without visible fat from homogeneous clear cell renal cell carcinoma. Eur Radiol 2019;30:1274–1284. doi:10.1007/s00330-019-06427-x.
[26] Jiang Y, Chen C, Xie J, Wang W, Zha X, Lv W, *et al*. Radiomics signature of computed tomography imaging for prediction of survival and chemotherapeutic benefits in gastric cancer. EBioMedicine 2018;36:171–182. doi:10.1016/j.ebiom.2018.09.007.
[27] Mariani P, Dureau S, Savignoni A, Rouic LL, Levy-Gabriel C, Piperno-Neumann S, *et al*. Development of a prognostic nomogram for liver metastasis of uveal melanoma patients selected by liver MRI. Cancers (Basel) 2019;11(6):863. doi:10.3390/cancers11060863.
[28] Yuan C, Wang Z, Gu D, Tian J, Zhao P, Wei J, *et al*. Prediction early recurrence of hepatocellular carcinoma eligible for curative ablation using a Radiomics nomogram. Cancer Imaging 2019;19:21. doi:10.1186/s40644-019-0207-7.